Journal of Organometallic Chemistry 696 (2011) 3593–3600

Contents lists available at SciVerse ScienceDirect

Journal of Organometallic Chemistry

journal homepage: www.elsevier.com/locate/jorganchem

Chemical behavior of *ortho*-hydroquinone-based bis(pyrazol-1-yl)methane ligands in the presence of palladium(II) chloride

Florian Blasberg, Michael Bolte, Matthias Wagner, Hans-Wolfram Lerner*

Institut für Anorganische Chemie, Goethe-Universität Frankfurt am Main, Max-von-Laue-Str. 7, 60438 Frankfurt am Main, Germany

ARTICLE INFO

Article history:
Received 31 May 2011
Received in revised form
1 July 2011
Accepted 1 August 2011

Keywords:
Bis(pyrazol-1-yl)methane
Pyrazole
Coordination chemistry
X-ray structure analysis

ABSTRACT

The synthesis, structural characterization, and coordination behavior of ditopic *ortho*-hydroquinone-based bis(pyrazol-1-yl)methane ligands (*ortho*-$(OH)_2C_6H_3$-4-$CHpz_2$, *ortho*-$(OH)_2C_6H_3$-4-$CH(3\text{-}Phpz)_2$, and *ortho*-$(OH)_2C_6H_3$-4-$CH(3\text{-}t\text{Bupz})_2$) with pyrazole, 3-phenylpyrazole, and 3-*tert*-butylpyrazole as donors are described. The reaction of a soluble $PdCl_2$-source with *ortho*-$(OH)_2C_6H_3$-4-$CHpz_2$ in acetonitrile yielded the related square-planar *N,N*-coordinated Pd(II) dichloride complex, whereas treatment of *ortho*-$(OH)_2C_6H_3$-4-$CH(3\text{-}Phpz)_2$ or *ortho*-$(OH)_2C_6H_3$-4-$CH(3\text{-}t\text{Bupz})_2$ with $PdCl_2$ in acetonitrile resulted in degradation of these ligands. The Pd(II) complexes *trans*-$(3\text{-}PhpzH)_2PdCl_2$ and *trans*-$(3\text{-}t\text{BupzH})_2PdCl_2$ were isolated and fully characterized including X-ray diffraction analyses.

1. Introduction

Multidentate ligand systems have attracted considerable interest in the last decades [1,2]. Prominent examples of this class of ligands are the (pyrazol-1-yl)borates (scorpionates) $[R_nBpz_{4-n}]^-$ (R = H, alkyl, aryl; $n = 2, 1, 0$; pz = pyrazol-1-yl) [3–5] and the (2-methimazol-1-yl)borates $[R_nBmt_{4-n}]^-$ (R = H, alkyl, aryl; $n = 2, 1, 0$; mt = 2-methimazol-1-yl) [6–8]. Especially scorpionates have found applications in a wide range of chemistry, from modeling the active site of metalloenzymes, through analytical chemistry and organic synthesis to catalysis and materials science [9].

However, in the presence of transition metal salts MX_2, in some cases we observed degradation reactions of scorpionate ligands [10]. Especially bis(pyrazol-1-yl)borates [11–13] such as the ones mentioned in Fig. 1 tend to decompose to give complexes of the metal with the corresponding pyrazole derivatives. To circumvent these problems, we decided to further investigate the properties of bis(pyrazol-1-yl)methanes as a potentially more stable neutral substitute for bis(pyrazol-1-yl)borates.

Since our group has a long-standing interest in the development of redox-active ligands based on *para*-hydroquinone (Fig. 2), both for use in homogeneous catalysis and in the assembly of coordination polymers and networks [14], we combined bis(pyrazol-1-yl)methane chelators with the redox-active *para*-hydroquinone unit, as shown in Fig. 2 and thoroughly investigated their coordination behavior, as well as their redox chemistry [14–17].

By the observation that the *para*-hydroquinone derivative A (Scheme 1) is oxidized to the *ortho*-benzoquinone B (Scheme 1), rather than to the expected *para*-benzoquinone derivative, we have also become interested in developing the chemistry of *ortho*-hydroquinone-based bis(pyrazol-1-yl)methane derivatives. Therefore we synthesized **1(H)**, **1(Ph)**, and **1(*t*Bu)** (Fig. 2), in order to make comparisons to their *para*-hydroquinone-based congeners.

The purpose of this paper is to describe the synthesis and characterization of the ditopic ligands **1(H)**, **1(Ph)**, and **1(*t*Bu)**, as well as their chemical behavior toward $PdCl_2$ as a transition metal role model. In addition the solid-state structures of the ligands **1(H)** and **1(*t*Bu)** and those of their reaction products with $PdCl_2$ will be reported herein.

2. Results and discussion

2.1. Synthesis of the ortho-hydroquinone-based bis(pyrazol-1-yl) methane ligands *1(H)*, *1(Ph)*, and *1(tBu)*

In a preceding report we have already noted the *ortho*-hydroquinone-based bis(pyrazol-1-yl)methane ligand **1(H)** [17], but synthetic details and analytical data of **1(H)** such as metric parameters will be discussed here. The bis(pyrazol-1-yl)methane **1(H)** was prepared in a three-step one-pot procedure (Scheme 2): (i) At first pyrazole was deprotonated with sodium hydride in THF. (ii) Then the so formed sodium pyrazolide reacted with $SOCl_2$ to

* Corresponding author. Tel.: +49 69 798 29152; fax: +49 69 798 29260.
E-mail address: lerner@chemie.uni-frankfurt.de (H.-W. Lerner).

0022-328X/$ – see front matter © 2011 Elsevier B.V. All rights reserved.
doi:10.1016/j.jorganchem.2011.08.002

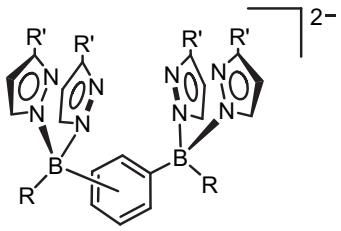

Fig. 1. A variety of ditopic (pyrazol-1-yl)borates (scorpionates).

produce the intermediate pz_2SO. (iii) Treatment of pz_2SO with 3,4-dihydroxybenzaldehyde and pyridine took place with concomitant liberation of SO_2 and gave **1(H)** in 54% isolated yield. The ^{1}H NMR spectrum (d_6-DMSO) revealed signals with the expected integral ratio of two pyrazol-1-yl groups and one *ortho*-hydroquinone unit. Resonances for the pyrazole groups are observed at 6.33 (pz-H4, for numbering see Scheme 2), 7.56, and 7.80 (pz-H3,5), whereas the bis(pyrazol-1-yl)methyl proton resonates downfield at 7.83 ppm. The signal of the hydroquinone H6 overlays with the resonance of pyrazole H4 to form a multiplet, but hydroquinone H2 and H5 both give well-resolved doublets at 6.52 ($^4J_{HH} = 1.9$ Hz) and 6.71 ppm ($^3J_{HH} = 8.2$ Hz), respectively. Finally the OH groups give rise to a broadened singlet at 9.11 ppm with the expected integral of 2 H. ^{13}C NMR data are as expected for this type of compounds and therefore do not merit further discussion.

When phenylpyrazole was applied as starting material the bis(pyrazol-1-yl)methane **1(Ph)** was obtained under identical reaction conditions as those described for the synthesis of **1(H)** (Scheme 2). This approach yielded the bis(pyrazol-1-yl)methane **1(Ph)** after column chromatography. In the ^{1}H NMR spectrum (d_6-DMSO) a ratio of one *ortho*-hydroquinone unit and one bis(3-phenylpyrazol-1-yl)methane fragment is found. Well-resolved signals of the aromatic protons appear at 6.48 (dd, $^3J_{HH} = 8.3$, $^4J_{HH} = 2.0$, HQ-H6), 6.66 (d, $^4J_{HH} = 2.0$, HQ-H2) as well as 6.76 ppm (d, $^3J_{HH} = 8.3$, HQ-H5), while the pyrazole protons H4 and H5 resonate at 6.84 and 7.94 ppm, respectively. The H nuclei of the phenyl substituents are found as multiplets in the range of 7.31–7.82 ppm, while the methine hydrogen atom resonates at 7.91 ppm. The ^{13}C NMR spectrum of **1(Ph)** comprises no particularity and is not further discussed here.

The same synthetic route as described for **1(H)** and **1(Ph)** was applied for the preparation of **1(*t*Bu)** (Scheme 2). Starting from 3-*tert*-butylpyrazole, **1(*t*Bu)** was obtained, albeit in a slightly lower yield (45%) compared to those of the synthesis of **1(H)** and **1(Ph)**. In this context it should be noted that optimization of the reaction conditions proved to be fruitless (e.g. use of 1–50 equivalents of pyridine, 1–24 h reaction time, use of $CoCl_2$ as a catalyst (classical Petterson reaction [18])). The ^{1}H NMR spectrum of **1(*t*Bu)** (d_6-DMSO) shows the expected signal pattern of a 3-substituted bis-(pyrazol-1-yl)methane with the pyrazole H4 resonating as a multiplet at 6.23 ppm, superimposed by H6 on the hydroquinone core, and the pyrazole-H5 as a multiplet together with the methine proton at 7.61 ppm. The *tert*-butyl substituents give rise to a singlet at 1.23 ppm and the remaining proton signals of the *ortho*-hydroquinone, H2 and H5, are observed at 6.42 (d, $^4J_{HH} = 1.7$ Hz) and 6.68 ppm (d, $^3J_{HH} = 8.2$ Hz), respectively. In the downfield region at 9.05 ppm the OH hydrogen atoms on the *ortho*-hydroquinone come to resonance. All these values show only minor shifts compared to the unsubstituted parent compound **1(H)** and the ^{13}C NMR spectrum shows no peculiarities and is therefore not discussed here.

2.2. Synthesis of the bis(pyrazol-1-yl)methane Pd(II) complex *2(H)*

The synthesis of complex **2(H)** is summarized in Scheme 3. Treatment of (cod)$PdCl_2$ (cod = 1,5-cyclooctadiene) with **1(H)** in HPLC-grade acetonitrile (in the presence of atmospheric moisture and oxygen) at reflux temperature resulted in the clean formation of the expected *N*,*N*-coordination complex **2(H)** (Scheme 3) in 87% yield. The elevated temperatures are necessary to ensure sufficient dissolution of **1(H)** in acetonitrile.

The ^{1}H NMR spectrum of **2(H)** in d_6-DMSO shows the expected signal pattern of a bis(pyrazol-1-yl)methane moiety as well as an *ortho*-hydroquinone unit. Most importantly the resonances of the OH groups are observed at 9.27 and 9.43 ppm, indicating *N*,*N*-coordination of $PdCl_2$. All protons on the pyrazole rings experience pronounced downfield shifts ranging from 0.36 (pz-H4, for numbering see Scheme 2) to 0.69 ppm upon coordination to the $PdCl_2$ fragment. This is however different for the hydroquinone

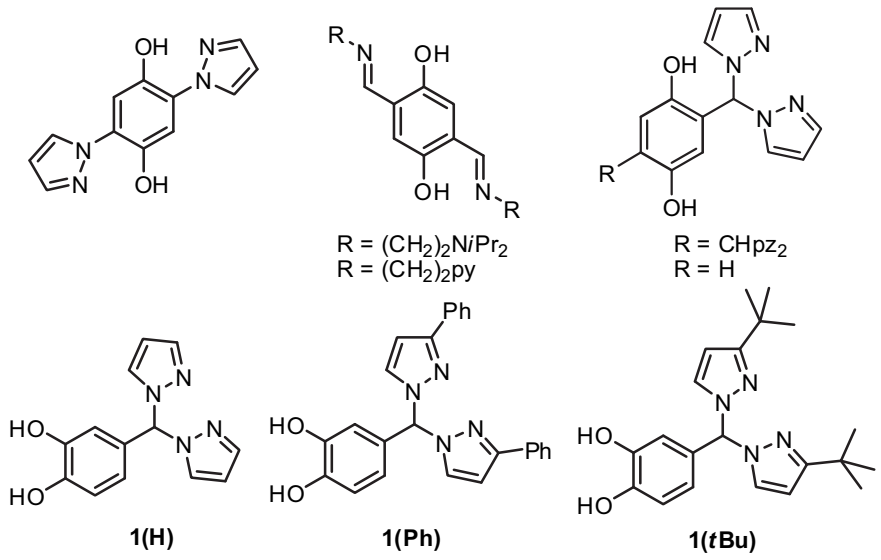

Fig. 2. Electroactive ligands based on 1,2- and 1,4-hydroquinone.

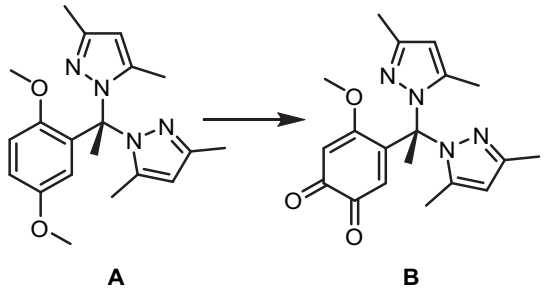

Scheme 1. Synthesis of an *ortho*-hydroquinone derivative B by reaction of a *para*-hydroquinone derivative A with $(NH_4)_2[Ce(NO_3)_6]$ in acetonitrile at r.t.

moiety of **2(H)**. While the chemical shift of HQ-H5 is unchanged, the other two hydrogen atoms on the aromatic core experience a significant highfield shift of ca. 0.5 ppm. The overall situation is well reproduced in the ^{13}C NMR spectrum of **2(H)** with pyrazole C3 and C5 showing the most pronounced downfield shift (4.2 and 5.8 ppm). Besides the product signals, another signal set (<10%), which can be attributed to the free ligand **1(H)**, is found in d_6-DMSO solution. This is, however, not observed in d_3-acetonitrile solution, showing that DMSO is a sufficiently strong donor to dissociate some Pd(II) cations from the bis(pyrazol-1-yl)methane chelators.

2.3. Reactivity of *1(Ph)* and *1(tBu)* toward $PdCl_2$

When the sterically more demanding derivatives **1(Ph)** and **1(*t*Bu)** were reacted with $PdCl_2$ in HPLC-grade acetonitrile at elevated temperature ($T = 82$ °C; without exclusion of atmospheric moisture and oxygen), the expected bis(pyrazol-1-yl)methane complexes analogous to **2(H)** were not formed. Instead, hydrolysis reactions of **1(Ph)** and **1(*t*Bu)** took place to give on the one hand 3,4-dihydroxybenzaldehyde (as monitored in the ^1H NMR spectrum of the reaction mixture) and on the other hand the Pd(II) complexes **3(Ph)** and **3(*t*Bu)** (Scheme 4). After recrystallization of the yellow-colored crude products, X-ray quality crystals of **3(Ph)** and **3(*t*Bu)** were isolated. The ^1H NMR spectra ($CDCl_3$) of both complexes feature the signal pattern of 3-substituted pyrazole moieties, with only minor shifts compared to the free pyrazoles. Importantly, resonances at 11.84 ppm (**3(Ph)**) and 11.33 ppm (**3(*t*Bu)**) were observed which can be assigned to the protons of free N–H units.

To ensure comparability to the synthesis of **2(H)**, reactions were in the beginning run for a similar time, but later on it was established, that hydrolysis to **3(Ph)** and **3(*t*Bu)** is fast, therefore a shorter reaction time was deemed sufficient.

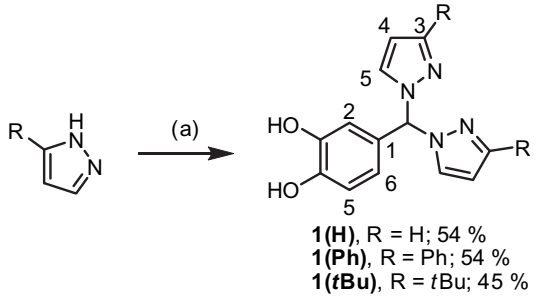

Scheme 2. Synthesis and numbering scheme of *ortho*-hydroquinone-based bis(pyrazol-1-yl)methane ligands **1(H)**, **1(Ph)**, and **1(*t*Bu)**. (a) (i) NaH, THF, 30 min; (ii) $SOCl_2$, THF, 5 min; (iii) 3,4-dihydroxybenzaldehyde, pyridine, THF, reflux, overnight.

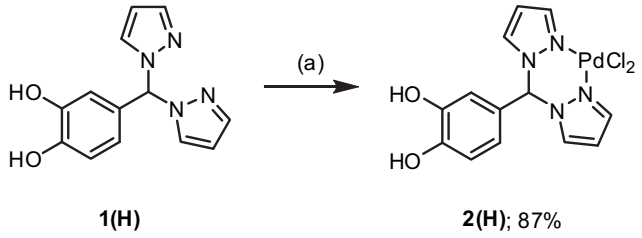

Scheme 3. Synthesis of Pd(II) complex **2(H)**. (a) $(cod)PdCl_2$, MeCN, reflux, 3 h.

In contrast to the reaction of hydroquinone derivative **1(H)** with $PdCl_2$, it is obviously not possible to synthesize the corresponding $PdCl_2$ complexes of the bis(pyrazol-1-yl)methanes **1(Ph)** and **1(*t*Bu)**, even though two examples of $PdCl_2$ complexes of sterically demanding bis(pyrazol-1-yl)methanes ($\{H_2C(3,5\text{-}Ad_2pz)_2\}PdCl_2$, [19] $\{Ph_2C(3\text{-}t\text{Bupz})_2\}PdCl_2$, [20]; Ad = adamantyl) are known. It is worth mentioning that $\{Ph_2C(3\text{-}t\text{Bupz})_2\}PdCl_2$ was prepared in CH_2Cl_2 and $\{H_2C(3,5\text{-}Ad_2pz)_2\}PdCl_2$ in CH_2Cl_2/MeOH solution without exclusion of atmospheric moisture or oxygen. So in both of these complexes coordination of $PdCl_2$ to a sterically encumbered bis(pyrazol-1-yl)methane is obviously possible without decomposition reactions caused by moisture or protic solvents. Since the free bis(pyrazol-1-yl)methane ligand of complex $\{Ph_2C(3\text{-}t\text{Bupz})_2\}PdCl_2$ appears to have an even higher steric demand, compared to **1(*t*Bu)**, steric bulk alone cannot be the deciding factor. As the preparation of free ligands **1(H)**, **1(Ph)**, and **1(*t*Bu)** includes aqueous workup, and no decomposition is observed during preparation, we can conclude that in the absence of Pd(II), all these *ortho*-hydroquinone-based bis(pyrazol-1-yl)methanes are water stable. However, when Pd(II) is present, hydrolysis of **1(Ph)** and **1(*t*Bu)** takes place rapidly. Thus the question arises as to what are the factors leading to decomposition. A marked difference between $Ph_2C(3\text{-}t\text{Bupz})_2$ and **1(tBu)** is obviously the hydroxyl substitution pattern of the latter. These oxygen atoms can exert two influences: (i) Mesomeric stabilization of a positive (partial) charge at the bis(pyrazol-1-yl) methane carbon atom by the *para*-hydroxyl group. (ii) Redox-assisted decomposition of the bis(pyrazol-1-yl)methane unit. A detailed study into the decomposition mechanism is subject of current investigation.

To clarify whether the presence of water poses a problem or whether the ligands **1(Ph)** and **1(*t*Bu)** are intrinsically unable to form Pd(II) complexes, NMR-scale experiments with rigorously dried solvents in flame-sealed NMR-tubes were conducted. A mixture of **1(Ph)** and $(cod)PdCl_2$ in d_8-THF shows only the signal sets of **1(Ph)** and a 1,5-cyclooctadiene ring. No change in the chemical shifts, even after prolonged time at room temperature, came about. Heating to 60 °C for 150 min also did not bring forth a change in the ^1H NMR spectrum. When the NMR tube was, however, heated to 120 °C for 90 min, a significant color change from yellow to brown was observed, as well as the deposition of

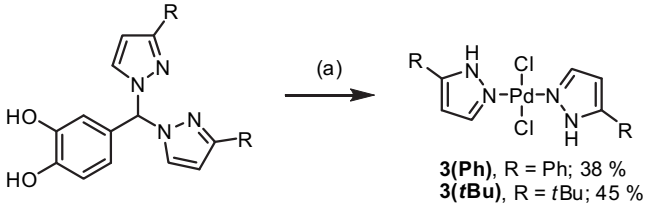

Scheme 4. Synthesis of **3(Ph)** and **3(*t*Bu)** by the reaction of $PdCl_2$ with **1(Ph)** and **1(*t*Bu)**, respectively. (a) $(MeCN)_2PdCl_2$, MeCN, reflux, 40 min (R = Ph) or 150 min (R = *t*Bu).

a black precipitate, which indicates that a redox reaction took place (in the literature it was reported that the parent *ortho*-quinone decomposes at temperatures higher than 70 °C to give a black insoluble material [21]).

To assure complete comparability with the experiments conducted in acetonitrile in the presence of water, another NMR-scale experiment, was carried out, but this time in absolute d_3-actonitrile. At 80 °C once again no reaction was observed, as monitored by ^{1}H NMR spectroscopy. At 95 °C a homogeneous solution formed, but the ^{1}H NMR spectrum recorded after 75 min at this temperature already showed significant decomposition. However, the spectroscopic signature of a Pd(II) complex related to **2(H)** was not observable. Further two hours heating at 95 °C led to the deposition of a black, insoluble residue, and even more pronounced decomposition was observed in the ^{1}H NMR spectrum of the reaction solution.

For the time being, we can conclude that the degradation of the *ortho*-hydroquinone-based bis(pyrazol-1-yl)methanes **1(Ph)** and **1(*t*Bu)** is caused by steric bulk and a yet undisclosed effect of the quinone backbone.

2.4. X-ray crystallographic structures

Single crystals of **1(H)** (orthorhombic space group *Fdd*2, Fig. 3, Table 1) were obtained by slow evaporation of a saturated chloroform solution. As already evidenced by the spectroscopic data, **1(H)** consists of a bis(pyrazol-1-yl)methane moiety and an *ortho*-hydroquinone unit with C–O-bond lengths of 1.372(6) Å and 1.378(7) Å, which compare favorably to the bond lengths in the corresponding *para*-hydroquinone system (2,5-$(OH)_2C_6H_3CH(pz)_2$: C–O = 1.368(3) Å and 1.374(3) Å [15]). The differences in the C–C-bond lengths of the six-membered ring (1.370(7) Å–1.403(7) Å) is only slightly more pronounced than in 2,5-$(OH)_2C_6H_3CH(pz)_2$ (1.384(3) Å–1.396(3) Å). When comparing the C–N bond lengths in **1(H)** (1.456(7) Å, 1.468(7) Å) with those of 2,5-$(OH)_2C_6H_3CH(pz)_2$ (1.455(3) Å, 1.464(3) Å) one can find virtually no differences and the same holds true for the N–C–N angle (110.4(4)°), which is close to the perfect tetrahedral angle. As is common for bis(pyrazol-1-yl) methane moieties the pyrazole donors adopt a conformation in which the nitrogen lone pairs point away from each other.

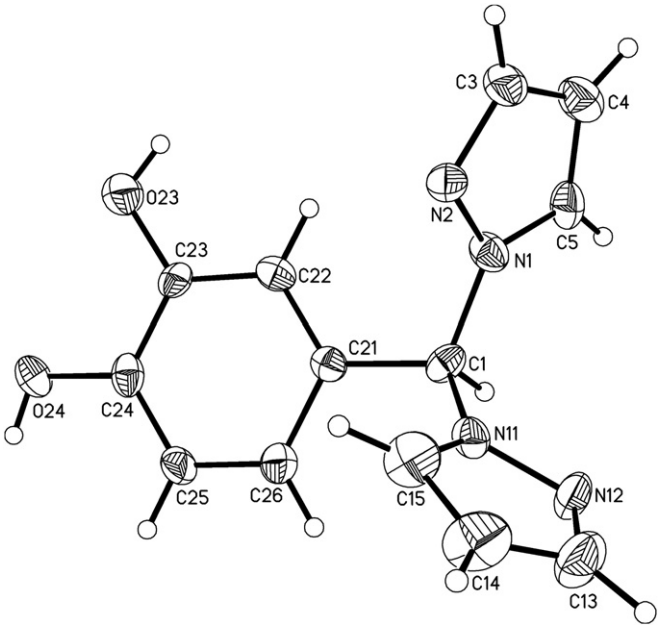

Fig. 3. Molecular structure of **1(H)** (50% displacement ellipsoids). Selected bond lengths (Å), bond angles (°), and torsion angles (°): C1–N1 1.468(7), C1–N11 1.456(7), C1–C21 1.504(8), C23–O23 1.378(7), C24–O24 1.372(6); N1–C1–C21 113.2(4), N11–C1–C21 112.5(4), N11–C1–N1 110.4(4); C21–C1–N1–N2 61.1(6), C21–C1–N11–N12 144.0(4).

Single crystals of **1(*t*Bu)** (monoclinic space group *C*2/c, Fig. 4, Table 1) were obtained by layering an EtOAc solution of **1(*t*Bu)** with hexane. As already deduced from the NMR spectrum, **1(*t*Bu)** features a bis(pyrazol-1-yl)methane moiety attached in position 1 to a 3,4-dihydroxybenzene unit. When compared to the unsubstituted parent compound **1(H)** (cf. Fig. 1), only slight differences in bond lengths as well as angles can be observed. The most significant difference is observed for the C1–C21 bond between the bis(pyrazol-1-yl)methane fragment and the *ortho*-hydroquinone moiety, which is slightly elongated (1.522(4) Å) compared to the length of 1.504(8) Å of **1(H)**. When also considering the substituted *para*-hydroquinonyl bis(pyrazol-1-yl)methanes (2,5-$(OCH_3)_2$-C_6H_3CH(3-Mepz)$_2$ 1.513(2) Å, 2,5-$(OCH_3)_2$-C_6H_3CH(3-Phpz)$_2$ 1.521(3) Å, 2,5-$(OCH_3)_2$-C_6H_3CH(3,5-Me_2pz)$_2$ 1.522(2) Å, 2,5-$(OCH_3)_2$-C_6H_3CH(3-*t*Bupz)$_2$ 1.525(2) Å) [17], a correlation between the steric bulk of the pyrazole donors and the bond length of the carbon atoms connecting the bis(pyrazol-1-yl)methane fragment and the aromatic ring can be found. The C–O bond farthest away from the bis(pyrazol-1-yl)methane group (C24–O24 = 1.386(4) Å) in **1(*t*Bu)** is slightly elongated compared to the other C–O bond in **1(*t*Bu)** (C23–O23 = 1.378(4) Å) and the two C–O bonds in **1(H)** (C23–O23 = 1.378(7) Å, C24–O24 = 1.372(6) Å; Fig. 3), probably due to inductive electronic effects.

The Pd(II) complex **2(H)** crystallizes from a saturated THF solution by layering with hexane in the monoclinic space group $P2_1/n$ (Fig. 5). As expected, a square-planar *cis*-$PdCl_2$ fragment coordinated to the bis(pyrazol-1-yl)methane unit is found. All Pd–N bond lengths (Pd1–N2 = 2.007(3) Å, Pd1–N12 = 2.023(4) Å) are well comparable with those in other bis(pyrazol-1-yl)methane complexes (e.g. $(CH_3)_2C(pz)_2PdCl_2$ = 2.018(3) Å, 2030(3) Å) [22], which is also true for the Pd–Cl bond lengths (Pd1–Cl1 = 2.295(1) Å, Pd1–Cl2 = 2.287(1) Å). The Pd atom is in proximity of the π face of the aromatic core with a distance of 4.43 Å to the centroid. In this context it should be noted that the same feature was also found in the related naphtobenzoquinonyl bis(pyrazol-1-yl)methane palladium dichloride complex [16].

The molecular structures of the complexes **3(Ph)** and **3(*t*Bu)** are shown in Figs. 6 and 7. Selected bond lengths and angles are listed in the corresponding figure captions and details of the crystal structure analyses are summarized in Table 1.

3(Ph) crystallized from a hot acetonitrile solution upon cooling to room temperature in the triclinic space group $P-1$ (Fig. 6, Table 1). Two independent molecules are found in the asymmetric unit, which differ only slightly in their bond lengths, therefore only one molecule is discussed here. The Pd(II) d^8-ion lies on an inversion center (symmetry operations to generate equivalent atoms B: $-x+1$, $-y+1$, $-z$) and adopts a *trans*-square-planar geometry with two chloride and two 3-phenylpyrazole ligands. The Cl1–Pd1–N1 angle (89.71(4)°) is essentially 90° and the Pd1–N1 distance (2.022(1) Å) lies in the usual range of Pd–N bond interactions [15]. Similarly the Pd–Cl bond length (Pd1–Cl1 = 2.3004(8) Å) lies also in the expected range, while the pyrazole plane (N1–N2–C3–C4–C5) is almost coplanar to the Cl1–N1B–Cl1B plane, due to N–H···Cl interactions (Cl1···H2 = 2.400 Å).

In contrast to **3(Ph)**, the *t*Bu-substituted complex **3(*t*Bu)** crystallized from acetonitrile (monoclinic space group $P2_1/c$) as a hydrogen-bridged dimer together with 1.5 equivalents of MeCN (Fig. 7, Table 1). With a bond length of 2.006(5) Å for Pd1–N1 and 1.997(5) Å for Pd1–N11 the palladium nitrogen bonds are slightly

Table 1
Selected crystallographic data and structure refinement details for **1(H)**, **1(*t*Bu)**, **2(H)**, **3(Ph)**, and **3(*t*Bu)**.

Compound	**1(H)**	**1(*t*Bu)**	**2(H)**	**3(Ph)**	**3(*t*Bu)**
Formula	$C_{13}H_{12}N_4O_2$	$C_{21}H_{28}N_4O_2$	$C_{13}H_{12}Cl_2N_4O_2Pd$	$C_{18}H_{16}Cl_2N_4Pd$	$C_{14}H_{24}Cl_2N_4Pd \times 0.75$ MeCN
f_w	256.27	368.47	433.57	465.65	456.46
Color, shape	Colorless, needle	Colorless, needle	Orange, needle	Brown yellow, plate	Light brown, block
Temp (K)	173(2)	173(2)	173(2)	173(2)	173(2)
Radiation	MoK$_\alpha$, 0.71073 Å	MoK$_\alpha$, 0.71073 Å	MoK$_\alpha$, 0.71073 Å	MoK$_\alpha$, 0.71073 Å	MoK$_\alpha$, 0.71073 Å
Crystal system	Orthorhombic	Monoclinic	Monoclinic	Triclinic	Monoclinic
Space group	*Fdd*2	*C*2/*c*	$P2_1/n$	$P-1$	$P2_1/c$
a (Å)	22.584(4)	26.827(5)	8.9894(5)	8.7050(17)	9.1023(3)
b (Å)	26.976(4)	9.4657(9)	13.7925(11)	9.3650(19)	37.7552(12)
c (Å)	8.1396(15)	16.918(3)	12.5055(8)	12.347(3)	12.3566(4)
$_\alpha$ (deg)	90	90	90	79.89(3)	90.00
β (deg)	90	100.983(14)	105.974(5)	87.53(3)	100.591(2)
γ (deg)	90	90	90	64.77(3)	90.00
V (Å^3)	4958.9(15)	4217.4(12)	1490.64(17)	895.8(3)	4174.1(2)
Z	16	8	4	2	8
$D_{calcd.}$ (g cm^{-3})	1.373	1.161	1.932	1.726	1.453
F(000)	2144	1584	856	464	1860
μ (mm^{-1})	0.097	0.076	1.614	1.342	1.151
Cryst size (mm)	0.16 × 0.09 × 0.09	0.33 × 0.07 × 0.07	0.28 × 0.09 × 0.09	0.40 × 0.30 × 0.15	0.23 × 0.23 × 0.21
No of rflns coll	5737	16,612	12,405	16,992	33,951
No of indep rflns (R_{int})	1248 (0.1340)	3715 (0.1681)	2778 (0.0955)	4993 (0.0379)	7311 (0.0745)
Data/restr/params	1248/1/174	3715/2/252	2778/2/212	4993/0/238	7311/0/429
GOOF on F^2	0.816	0.829	0.891	1.046	1.135
*R*1, *wR*2 ($I > 2\sigma(I)$)	0.0516, 0.0879	0.0581, 0.0973	0.0329, 0.0677	0.0231, 0.0592	0.0535, 0.1417
*R*1, *wR*2 (all data)	0.0946, 0.0993	0.1420, 0.1203	0.0542, 0.0727	0.0246, 0.0601	0.0678, 0.1471
Largest diff peak and hole (e Å^{-3})	0.392, −0.217	0.176, −0.213	0.611, −0.651	0.684, −0.691	1.570, −0.755

shorter than in **3(Ph)**, but still comparable to similar complexes. The Pd–Cl bond lengths (2.307(2) Å, 2.299(1) Å) in contrast show almost no deviation when compared to the Pd–Cl bond length in **3(Ph)**. Once again the chloro substituents on palladium are engaged in hydrogen bonds with the N–H moieties of a second molecule. However, this time there are four intermolecular hydrogen bonds that lead to the formation of dimers of **3(*t*Bu)**. In these dimers there is a short Pd1···Pd1A contact (3.442 Å), which is similar to the sum of the van der Waals radii of two Pd(II) ions [23]. Similar Pd(II)–Pd(II) short contacts have already been observed [24], but are not very common.

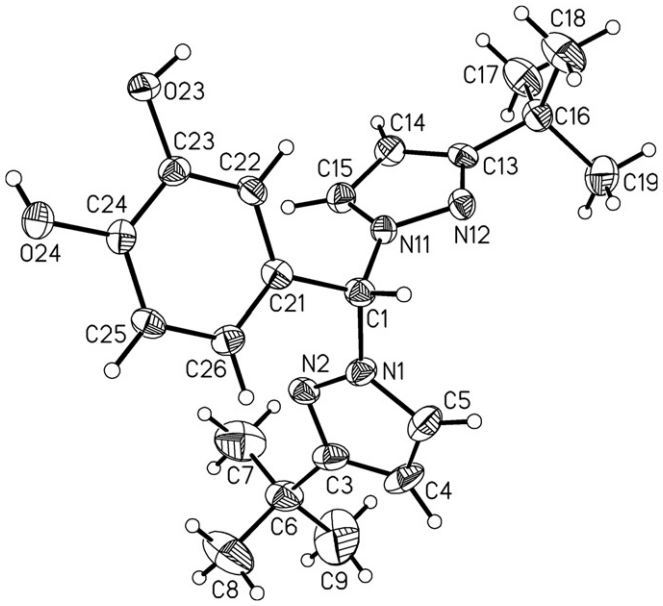

Fig. 4. Molecular structure of **1(*t*Bu)** (50% displacement ellipsoids). Selected bond lengths (Å), bond angles (°), and torsion angles (°): C1–N1 1.470(4), C1–N11 1.455(4), C1–C21 1.522(4), C23–O23 1.378(4), C24–O24 1.386(4); N1–C1–C21 113.2(3), N11–C1–C21 113.3(3), N11–C1–N1 110.4(3); C21–C1–N1–N2 53.2(4), C21–C1–N11–N12 135.6(3).

3. Experimental

NaH was used as 60% per weight suspension in mineral oil (commercially available); however, throughout the experimental part of this paper, all weight-out quantities refer to neat NaH. 3-*tert*-Butylpyrazole was prepared according to a published procedure [25]. All other chemicals were purchased from commercial suppliers and used as received.

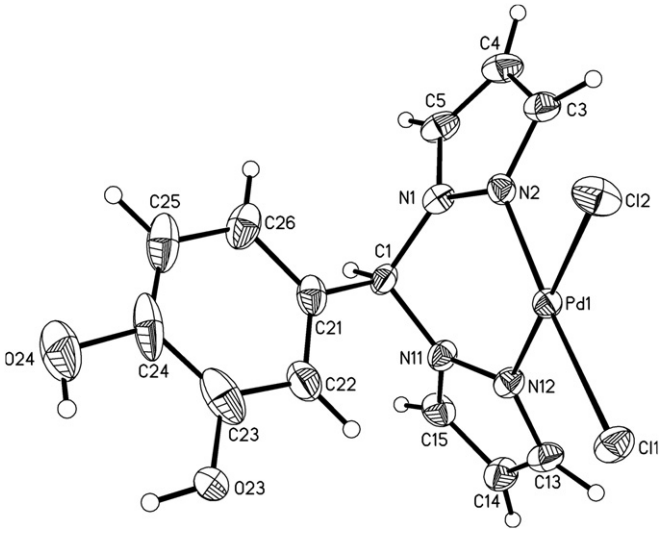

Fig. 5. Molecular structure of **2(H)** (50% displacement ellipsoids). Selected bond lengths and distances (Å), bond angles (°), and torsion angles (°): Pd1–N2 2.007(3), Pd1–N12 2.023(4), Pd1–Cl1 2.295(1), Pd1–Cl2 2.287(1), C1–N1 1.449(6), C1–N11 1.455(5), C1–C21 1.523(6), C23–O23 1.330(6), C24–O24 1.369(7), Pd1-COG(HQ) 4.34; N2–Pd1–N12 89.4(1), N1–C1–C21 113.8(4), N11–C1–C21 113.2(4), N11–C1–N1 109.3(4); N1–N2–Pd1–Cl2 −156.7(3), N11–N12–Pd1–Cl1 156.5(3), C21–C1–N1–N2 65.9(5), C21–C1–N11–N12 −70.4(5).

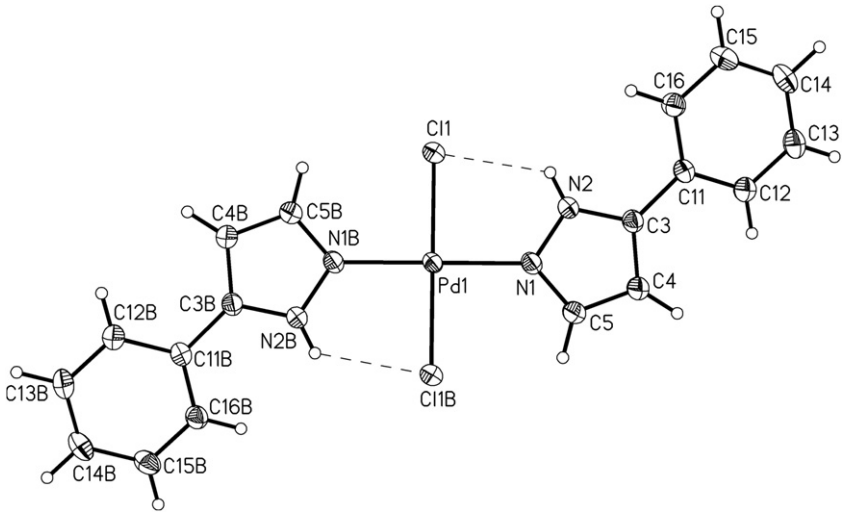

Fig. 6. Molecular structure of **3(Ph)** (50% displacement ellipsoids). Selected bond lengths and distances (Å), bond angles (°), and torsion angles (°): Pd1–Cl1 2.3004(8), Pd1–N1 2.022(1), N1–N2 1.360(2), N2–H2 0.81(2); Cl1–Pd1–N1 89.71(4); Cl1–Pd1–N1–N2 9.80(11), N2–C3–C11–C16 15.4(2). Symmetry operations to generate equivalent atoms B: $-x+1$, $-y+1$, $-z$.

NMR spectra were recorded with Bruker AM-250, Bruker Avance-300, and Bruker Avance-400 spectrometers. Chemical shifts are referenced to the residual solvent signal ($^1H/^{13}C\{^1H\}$: d_6-DMSO: 2.50/39.52; $CDCl_3$: 7.26/77.16). Abbreviations: s = singlet; d = doublet; dd = doublet of doublets; m = multiplet; pz = pyrazol-1-yl.

Elemental analyses were performed by the Microanalytical Laboratory of the University of Frankfurt. Mass spectra were recorded with a VG PLATFORM II mass spectrometer.

3.1. Synthesis of ***1(H)***

Neat pyrazole (2.00 g, 29.4 mmol) was added to NaH (0.71 g, 29.6 mmol) slurried in THF. $SOCl_2$ (1.07 mL, 1.75 g, 14.7 mmol) was added in one portion after 30 min and after another 5 min 3,4-dihydroxybenzaldehyde (2.03 g, 14.7 mmol), and pyridine (11.88 mL, 11.64 g, 147.2 mmol) were added and the resulting cloudy reaction mixture was heated to reflux overnight. H_2O (50 mL) was added and the aqueous phase extracted into CH_2Cl_2 (3×50 mL). The combined organic extracts were washed with brine, dried over $MgSO_4$, filtered, and the filtrate was evaporated to dryness *in vacuo*. The crude oily product was dissolved in EtOAc and the solution evaporated to dryness in order to remove residual pyridine. This procedure was repeated two to three times until brown lumps remained. $CHCl_3$ was added and the glass vessel agitated in an ultrasonic bath for 10 min in order to obtain finely divided particles. The resulting suspension was heated to reflux for 10 min. The insoluble colorless solid was isolated by filtration and dried under dynamic vacuum. Single crystals were obtained by slowly letting the saturated chloroform washings evaporate Yield: 2.02 g (54%). ^1H NMR (250.1 MHz, d_6-DMSO) $\delta = 6.33$ (m, 3 H; pz-H4, HQ-H6), 6.52 (d, $^4J_{HH} = 1.9$ Hz, 1 H; HQ-H2), 6.71 (d, $^3J_{HH} = 8.2$ Hz, 1 H; HQ-H5), 7.56, 7.80 ($2 \times$ d, $^3J_{HH} = 1.2$ Hz, 2.2 Hz, 2×2 H; pz-H3,5), 7.83 (s, 1 H; CH), 9.11 (s, 2 H; OH). ^{13}C NMR (62.9 MHz, d_6-DMSO) $\delta = 76.2$ (Cpz_2), 105.8 (pz-C4), 114.4 (HQ-C2), 115.3 (HQ-C5), 118.0 (HQ-C6), 127.5 (HQ-C1), 130.0, 139.7 (pz-C3,5), 145.2, 145.9 (HQ-C3,4). ESI–MS: m/z (%) = 255 $[M-H]^-$ (100). Anal. Calcd for $C_{13}H_{12}N_4O_2$ [256.27]: C 60.93, H 4.72, N 21.86. Found: C 60.70, H 4.73, N 22.12.

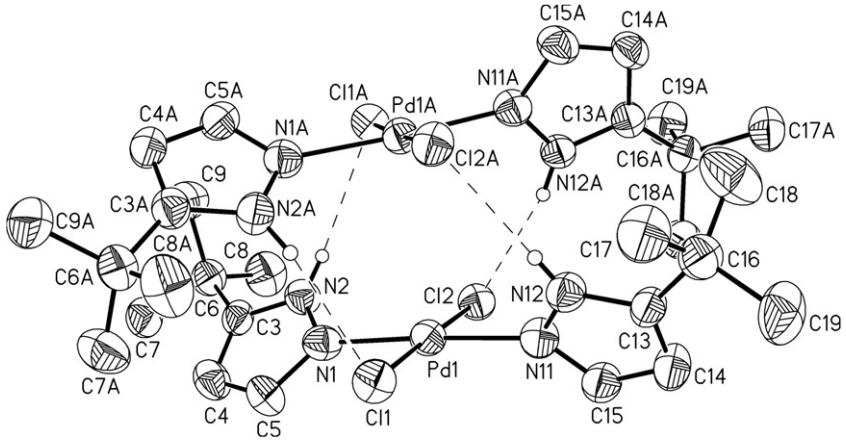

Fig. 7. Molecular structure of **3(*t*Bu)** (50% displacement ellipsoids). Selected bond lengths and distances (Å), bond angles (°), and torsion angles (°): Pd1–Cl1 2.307(2), Pd1–Cl2 2.299(1), Pd1–N1 2.006(5), Pd1–N11 1.997(5), N1–N2 1.355(7), N11–N12 1.342(7), N2–H2 0.85(6); N1–Pd1–Cl1 90.5(1), N1–Pd1–Cl2 89.8(1), N11–Pd1–Cl1 89.8(1), N11–Pd1–Cl2 89.8(1), Cl2–Pd1–Cl1 178.68(6), N1–Pd1–N11 177.1(2); Cl1–Pd1–N1–N2 148.9(4), Cl2–Pd1–N1–N2 −32.4(4), Cl1–Pd1–N11–N12 −58.6(4), Cl2–Pd1–N11–N12 122.7(4).

3.2. Synthesis of **1(Ph)**

3-Phenylpyrazole (2.00 g, 13.87 mmol) as a solid was added to a stirred slurry of NaH (0.33 g, 13.87 mmol) in THF (60 mL) at r.t. After 30 min $SOCl_2$ (0.50 mL, 0.83 g, 6.94 mmol) was added in one portion via syringe and the resulting mixture stirred at r.t. for 5 min. After addition of 3,4-dihydroxybenzaldehyde (0.96 g, 6.94 mmol) and pyridine (5.60 mL, 4.78 g, 60.40 mmol), the reaction mixture was kept at reflux temperature for 16 h. H_2O (50 mL) was added and the aqueous phase extracted into CH_2Cl_2 (3×50 mL). The combined organic extracts were washed with brine, dried over $MgSO_4$, filtered, and the filtrate was evaporated to dryness *in vacuo*. The crude product was purified by column chromatography (silica gel; $CHCl_3$/EtOAc 1:1). All product-containing fractions were concentrated by rotary evaporation at 40 °C and upon cooling to r.t. colorless **1(Ph)** precipitated, which was isolated by filtration and washed with Et_2O. Yield: 1.53 g (54%). $R_f = 0.63$ (silica gel, $CHCl_3$/EtOAc 1:1). ^{1}H NMR (400.1 MHz, d_6-DMSO) $\delta = 6.48$ (dd, $^3J_{HH} = 8.3$, $^4J_{HH} = 2.0$, 1 H; HQ-H6), 6.66 (d, $^4J_{HH} = 2.0$, 1 H; HQ-H2), 6.76 (d, $^3J_{HH} = 8.3$, 1 H; HQ-H5), 6.84 (d, $^3J_{HH} = 2.5$, 2 H; pz-H4), 7.31 (m, 2 H; Ph-H4), 7.41 (m, 4 H; Ph-H3), 7.82 (m, 4 H; Ph-H2), 7.91 (s, 1 H; CH), 7.94 (d, $^3J_{HH} = 2.5$, 2 H; pz-H5), 9.15 (bs, 2 H; OH). ^{13}C NMR (100.6 MHz, d_6-DMSO) $\delta = 76.7$ (Cpz_2), 103.5 (pz-C4), 114.4 (HQ-C2), 115.5 (HQ-C5), 118.2 (HQ-C6), 125.3 (Ph-C2), 127.2 (HQ-C1), 127.8 (Ph-C4), 128.7 (Ph-C3), 131.9 (pz-C5), 132.8 (Ph-C1), 145.3, 146.1 (HQ-C3,4), 151.0 (pz-C3). ESI–MS: *m*/*z* (%) 263 (67) $[M - Phpz]^-$, 408 (100) $[M - H]^-$. Anal. Calcd (%) for $C_{25}H_{20}N_4O_2$ (408.45): C 73.51, H 4.94, N 13.72. Found: C 73.22, H 4.86, N 13.67.

3.3. Synthesis of **1(tBu)**

Neat 3-*tert*-butylpyrazole (3.17 g, 25.52 mmol) was added to a stirred suspension of NaH (0.61 g, 25.52 mmol) in THF (70 mL). Stirring was continued for 30 min, then neat $SOCl_2$ (0.93 mL, 1.52 g, 12.76 mmol) was added in one portion via syringe. After treatment with 3,4-dihydroxybenzaldehyde (1.76 g, 12.76 mmol) and pyridine (10.30 mL, 10.09 g, 127.59 mmol), the reaction mixture was kept at reflux temperature for 16 h. H_2O (50 mL) was added and the aqueous phase extracted into CH_2Cl_2 (3×50 mL). The combined organic extracts were dried over $MgSO_4$, filtered, and the filtrate was evaporated to dryness *in vacuo*. The crude product was purified by column chromatography (silica gel; hexane/EtOAc 1:1). Yield: 2.13 g (45%). Single crystals were grown by layering an EtOAc solution of **1(*t*Bu)** with hexane. $R_f = 0.48$ (silica gel, hexane/EtOAc 1:1). ^{1}H NMR (250.1 MHz, d_6-DMSO) δ 1.23 (s, 18 H; CH_3), 6.23 (m, 3 H; pz-H4, HQ-H6), 6.42 (d, $^4J_{HH} = 1.7$, 1 H; HQ-H2), 6.68 (d, $^3J_{HH} = 8.2$, 1 H; HQ-H5), 7.61 (m, 3 H; pz-H5, CH), 9.05 (bs, 2 H; OH). ^{13}C NMR (62.9 MHz, d_6-DMSO) δ 30.4 (CH_3), 31.7 (CCH_3), 76.4 (Cpz_2), 102.2 (pz-C4), 114.2 (HQ-C2), 115.2 (HQ-C5), 117.7 (HQ-C6), 128.5 (HQ-C1), 130.0 (pz-C5), 145.1, 145.7 (HQ-C3,4), 161.2 (pz-C3). ESI–MS: *m*/*z* (%) 245 (100) $[M - t\text{Bupz}]^+$, 369 (56) $[M + H]^+$, 739 (11) $[M_2 + H]^+$. Anal. Calcd (%) for $C_{21}H_{28}N_4O_2$ (368.47): C 68.45, H 7.66, N 15.21. Found: C 68.93, H 7.46, N 15.18. IR (KBr): $\tilde{\nu}$ (cm^{-1}) 3121 (m), 2959 (m), 1610 (s), 1440 (m), 1294 (m), 1271 (s), 1195 (m), 1119 (s), 1069 (s), 1057 (m), 809 (s), 793 (m).

3.4. Synthesis of **2(H)**

In MeCN (20 mL) **1(H)** (0.47 g, 1.83 mmol) and (cod)$PdCl_2$ (0.55 mg, 1.93 mmol) were suspended and heated to reflux for 3 h. After cooling to r.t. all volatiles were removed *in vacuo* and the residue was washed with CH_2Cl_2 until the filtrate was colorless to yield a yellow solid. Single crystals of **2(H)** were obtained by layering a saturated THF solution with hexane. Yield: 0.69 g (87%). ^{1}H NMR (250.1 MHz, d_6-DMSO) δ 5.81 (dd, $^3J_{HH} = 8.2$, $^4J_{HH} = 1.7$, 1 H; HQ-H6), 5.99 (d, $^4J_{HH} = 1.7$, 1 H; HQ-H2), 6.69 (vt, $^3J_{HH} = 2.2$, 2 H; pz-H4), 6.81 (d, $^3J_{HH} = 8.2$, 1 H; HQ-H5), 8.05 (d, $^3J_{HH} = 2.2$, 2 H; pz-H3/5), 8.42 (s, 1 H; CH), 8.49 (d, $^3J_{HH} = 2.2$, 2 H; pz-H3/5), 9.27, 9.43 ($2 \times$ s, 2×1 H; OH). ^{13}C NMR (62.9 MHz, d_6-DMSO) δ 74.1 (Cpz_2), 107.3 (pz-C4), 112.5 (HQ-C2), 115.8 (HQ-C6), 116.2 (HQ-C5), 125.8 (HQ-C1), 135.8, 143.9 (pz-C3,5), 145.8, 146.6 (HQ-C3,4). ESI–MS *m*/*z* (%) 433 (100) $[M - H]^-$. Anal. Calcd for $C_{13}H_{12}Cl_2N_4O_2Pd \times 0.5\ H_2O$ (433.59 + 9.00): C 35.28, H 2.96, N 12.66. Found C 35.39, H 2.70, N 12.58. IR (KBr): $\tilde{\nu}$ (cm^{-1}) 1605 (w), 1518 (s), 1458 (w), 1326 (s), 1214 (m), 1183 (m), 1150 (w), 1118 (s), 1082 (m), 1074 (s), 1007 (w), 833 (w), 790 (s), 767 (s), 620 (m).

3.5. Reaction of **1(Ph)** with $PdCl_2$

1(Ph) (35 mg, 0.086 mmol) and $(MeCN)_2PdCl_2$ (22 mg, 0.086 mmol) in MeCN (3 mL) were heated to reflux for 40 min. The reaction mixture was evaporated to dryness and redissolved in boiling MeCN. Cooling to r.t. afforded orange plates of **3(Ph)** suitable for X-ray diffraction. Yield 15 mg (38%). ^{1}H NMR (250.1 MHz, $CDCl_3$) $\delta = 6.48$ (vt, $^3J_{HH} = 2.4$, 2 H; pz-H4), 7.39–7.56 (m, 10 H; Ph-H), 8.05 (vt, $^3J_{HH} = 2.4$, 2 H; pz-H5), 11.84 (s, 2 H; NH). ^{13}C NMR (62.9 MHz, $CDCl_3$) $\delta = 104.0$ (pz-C4), 126.0, 127.5, 129.5, 130.1 (Ph-C), 143.5 (pz-C5), 144.8 (pz-C3). ESI–MS: *m*/*z* (%) 321 (15) [(Phpz)$PdCl_2$]$^-$, 464 (5) $[M - H]^-$. Anal. Calcd (%) for $C_{18}H_{16}Cl_2N_4Pd$ (465.67): C 46.43, H 3.46, N 12.03. Found: C 46.24, H 3.48, N 12.12.

3.6. Reaction of **1(tBu)** with $PdCl_2$

1(*t*Bu) (50 mg, 0.136 mmol) and $(MeCN)_2PdCl_2$ (35 mg, 0.136 mmol) were combined in MeCN (2 mL) and heated to reflux for 2.5 h. The solution was concentrated by rotary evaporation. Upon cooling to r.t. cocrystals of **3(*t*Bu)** $\times$ 0.75 MeCN suitable for X-ray diffraction formed along with an oily residue. For purification the whole material was dissolved in hot MeCN and the resulting solution cooled to −30 °C for 2 days. Orange needles of analytically pure **3(*t*Bu)** were separated from the mother liquor and dried under a vacuum. Yield 26 mg (45%). ^{1}H NMR (300.0 MHz, $CDCl_3$) $\delta = 1.31$ (s, 18 H; CH_3), 6.08 (vt, $^3J_{HH} = 2.4$, 2 H; pz-H4), 7.91 (vt, $^3J_{HH} = 2.4$, 2 H; pz-H5), 11.33 (s, 2 H; NH). ^{13}C NMR (75.4 MHz, $CDCl_3$) $\delta = 29.9$ (CCH_3), 31.6 (CCH_3), 103.0 (pz-C4), 142.5 (pz-C5), 155.0 (pz-C3). ESI–MS: *m*/*z* (%) 213 (96) $[M - 2H]^-$, 301 (100) $[M - H - t\text{BupzH}]^-$, 426 (10) $[M - H]^-$. Anal. Calcd (%) for $C_{14}H_{24}Cl_2N_4Pd$ (425.69): C 39.50, H 5.68, N 13.16. Found: C 39.10, H 5.36, N 13.36.

3.7. Crystal structure determination

Data collection: STOE IPDS II two-circle diffractometer, graphite-monochromated MoK_α radiation ($\lambda = 0.71073$ Å, $T = 173(2)$ K). Empirical absorption corrections were performed using MULABS option in PLATON [26]. The structures were solved by direct methods using the program SHELXS [27] and refined against F^2 with full-matrix least-squares techniques using the program SHELXL-97 [28]. All non-hydrogen atoms were refined with anisotropic displacement parameters. Hydrogen atoms were located by difference Fourier synthesis and refined using a riding model.

Acknowledgments

M.W. is grateful to the "Deutsche Forschungsgemeinschaft" (DFG) for financial support (TR 49). F.B. wishes to thank the "Fonds der Chemischen Industrie" (FCI) for a Ph.D. grant.

Appendix A. Supplementary material

CCDC 826015, 826017, 826016, 826018 and 826019 contain the supplementary crystallographic data for this paper. These data can be obtained free of charge from The Cambridge Crystallographic Data Centre via www.ccdc.cam.ac.uk/data_request/cif.

References

[1] C. Bianchini, C. Mealli, A. Meli, I. Bernal (Eds.), Stereochemistry of Organometallic and Inorganic Compounds, Elsevier, Amsterdam, 1986, p. 146.
[2] K. Ruth, M. Müller, M. Bolte, J.W. Bats, M. Wagner, H.-W. Lerner, Z. Anorg. Allg. Chem. 633 (2007) 1485–1489.
[3] S. Trofimenko, Chem. Rev. 93 (1993) 943–980.
[4] S. Trofimenko, J. Am. Chem. Soc. 89 (1967) 3170–3177.
[5] S. Trofimenko, Scorpionates – The Coordination Chemistry of Polypyrazolylborate Ligands. Imperial College Press, London, 1999.
[6] L.F. Soares, D.C. Menezes, R.M. Silva, A.C. Doriguetto, J. Ellena, Y.P. Mascarenhas, E.E. Castellano, Polyhedron 23 (2004) 205–209.
[7] M. Garner, J. Reglinski, I. Cassidy, M.D. Spicer, A.R. Kennedy, Chem. Commun. (1996) 1975–1976.
[8] K. Kunz, M. Bolte, M. Wagner, H.-W. Lerner, Z. Anorg. Allg. Chem. 635 (2009) 1580–1584.
[9] R.D. Adams, F.A. Cotton (Eds.), Catalysis by Di- and Polynuclear Metal Cluster Complexes, Wiley, New York, 1988.
[10] S. Bieller, A. Haghiri, M. Bolte, J.W. Bats, M. Wagner, H.-W. Lerner, Inorg. Chim. Acta 359 (2006) 1559–1572.
[11] S. Bieller, F. Zhang, M. Bolte, J.W. Bats, H.-W. Lerner, M. Wagner, Organometallics 23 (2004) 2107–2113.
[12] F. Zhang, M. Bolte, H.-W. Lerner, M. Wagner, Organometallics 23 (2004) 5075–5080;
S. Bieller, M. Bolte, H.-W. Lerner, M. Wagner, Inorg. Chem. 44 (2005) 9489–9496;
F. Zhang, T. Morawitz, S. Bieller, M. Bolte, H.-W. Lerner, M. Wagner, Dalton Trans. (2007) 4594–4598;
T. Morawitz, M. Bolte, H.-W. Lerner, M. Wagner, Z. Anorg. Allg. Chem. 634 (2008) 1409–1414;
T. Morawitz, M. Bolte, H.-W. Lerner, M. Wagner, Z. Anorg. Allg. Chem. 634 (2008) 1570–1574.
[13] T. Morawitz, F. Zhang, M. Bolte, J.W. Bats, H.-W. Lerner, M. Wagner, Organometallics 27 (2008) 5067–5074.
[14] R. Dinnebier, H.-W. Lerner, L. Ding, K. Shankland, W.I.F. David, P.W. Stephens, M. Wagner, Z. Anorg. Allg. Chem. 628 (2002) 310–314;
G. Margraf, T. Kretz, F. Fabrizi de Biani, F. Laschi, S. Losi, P. Zanello, J.W. Bats, B. Wolf, K. Remović-Langer, M. Lang, A. Prokofiev, W. Assmus, H.-W. Lerner, M. Wagner, Inorg. Chem. 45 (2006) 1277–1288;
T. Kretz, J.W. Bats, S. Losi, B. Wolf, H.-W. Lerner, M. Lang, P. Zanello, M. Wagner, Dalton Trans. (2006) 4914–4921;
N.H. Phan, I. Halasz, I. Opahle, E. Alig, L. Fink, J.W. Bats, P.T. Cong, H.-W. Lerner, B. Sarkar, B. Wolf, H.O. Jeschke, M. Lang, R. Valentí, R. Dinnebier, M. Wagner, Cryst. Eng. Commun. 13 (2011) 391–395.
[15] S. Scheuermann, T. Kretz, H. Vitze, J.W. Bats, M. Bolte, H.-W. Lerner, M. Wagner, Chem. Eur. J. 14 (2008) 2590–2601.
[16] S. Scheuermann, B. Sarkar, M. Bolte, J.W. Bats, H.-W. Lerner, M. Wagner, Inorg. Chem. 48 (2009) 9385–9392.
[17] F. Blasberg, J.W. Bats, M. Bolte, H.-W. Lerner, M. Wagner, Inorg. Chem. 49 (2010) 7435–7445.
[18] K.I. Thé, L.K. Peterson, Can. J. Chem. 51 (1973) 422–426;
K.I. Thé, L.K. Peterson, E. Kiehlmann, Can. J. Chem. 51 (1973) 2448–2451;
L.K. Peterson, E. Kiehlmann, A.R. Sanger, K.I. Thé, Can. J. Chem. 52 (1974) 2367–2374.
[19] M.W. Jones, R.M. Adlington, J.E. Baldwin, D.D. Le Pevelen, N. Smiljanic, Inorg. Chim. Acta 363 (2010) 1097–1101.
[20] S. Tsuji, D.C. Swenson, R.F. Jordan, Organometallics 18 (1999) 4758–4764.
[21] R. Willstätter, A. Pfannenstiel, Chem. Ber. 37 (1904) 4744–4746.
[22] G. Minghetti, M.A. Cinellu, A.L. Bandini, G. Banditelli, F. Demartin, M. Manassero, J. Organomet. Chem. 315 (1986) 387–399.
[23] T.W. Hambley, Inorg. Chem. 37 (1998) 3767–3774.
[24] A.J. Blake, A.J. Holder, Y.V. Roberts, M. Schröder, J. Chem. Soc., Chem. Commun. (1993) 260–262. K. Samochocka, I. Fokt, R. Anulewicz-Ostrowska, T. Przewloka, A.P. Mazurek, L. Fuks, W. Lewandowski, L. Kozerski, W. Bocian, E. Bednarek, H. Lewandowska, J. Sitkowski, W. Priebe, Dalton Trans. (2003) 2177–2183.
[25] S. Trofimenko, J.C. Calabrese, J.S. Thompson, Inorg. Chem. 26 (1987) 1507–1514.
[26] A.L. Spek, Acta Crystallogr. A 46 (1990) C34.
[27] G.M. Sheldrick, Acta Crystallogr. A 46 (1990) 467–473.
[28] G.M. Sheldrick, SHELXL-97, A Program for the Refinement of Crystal Structures. University of Göttingen, Göttingen, Germany, 1997.